EUROfusion

WPBB-CPR(18) 20017

S Ruck et al.

Structured Cooling Channels for Intensively Heated Blanket Components

Preprint of Paper to be submitted for publication in Proceeding of
30th Symposium on Fusion Technology (SOFT)

This work has been carried out within the framework of the EUROfusion Consortium and has received funding from the Euratom research and training programme 2014-2018 under grant agreement No 633053. The views and opinions expressed herein do not necessarily reflect those of the European Commission.

Structured Cooling Channels for Intensively Heated Blanket Components

Sebastian Ruck, Frederik Arbeiter, Björn Brenneis, Christine Klein, Francisco Hernandez, Heiko Neuberger, Florian Schwab

[a]*Karlsruhe Institute of Technology, Eggenstein-Leopoldshafen, Germany*

The thermal hydraulics of helium-gas cooled channels for First Wall applications structured by truncated fully attached and semi-detached upward directed V-shaped ribs and spherical dimples were investigated. The rib-height-to-hydraulic-diameter ratio was $e/D_h = 0.1$, the rib-pitch-to-rib-height ratio was $p/e = 10$ and the gap-height-to-rib-height ratio for the semi-detached rib was $c/e = 0.1$. The dimples were positioned in a staggered array. The ratio of dimple depth to dimple print diameter was $D_d/d = 0.3$ and the distance between the dimple centers was $s_1 = 1.2$, 1.5 and 2.0 in streamwise direction and $s_2 = 1.5$ in spanwise direction. Large-Eddy-Simulations were performed and the global and local heat transfer coefficient, pressure drop and cooling performance were analyzed. It was found that the heat transfer coefficient ratio of the V-shaped ribs was in the range from 2.6 to 2.8. The semi-detached ribs provided the highest heat transfer and the best cooling performance. The dimpled structures increased the heat transfer by the factor of 1.3 to 1.4 without a significant pressure drop rise, but regions of heat transfer deterioration occur over each upstream dimple half.

Keywords: First Wall Cooling, Structured Cooling Channels, Semi-Detached V-Shaped Ribs, Dimpled Surface

1. Introduction

The upper and lower design temperature limits of the First Wall (FW) are defined by the steep reduction of mechanical strength of EUROFER for temperatures above 550 °C and the Ductile-to-Brittle-Transition-Temperature under irradiation of about 300 °C. Maximum temperatures in the EUROFER structure occur on the plasma-facing surface and depend on the wall heat flux generated by the plasma and on the helium cooling performance. Except unsteady power peaks of up to several MW/m^2 (which can appear accidently), uniform heat flux densities at the first wall can be expected in a range from 0.5 MW/m^2 to 1.0 MW/m^2 [1,2]. The low volumetric heat capacity and thermal conductivity (compared to liquid coolants) of helium-gas requires thermal-hydraulically improved surface designs for the cooling channels to enhance heat transfer and to ensure an operation within the temperature limits. Surface structuring in cooling channels of helium-gas cooled FW applications for heat transfer enhancement and their prospects of success in efficiency and effectiveness in terms of cooling performance were investigated for several thermal-hydraulic conditions and surface structure designs in the last years, i.e. Ruck and Arbeiter [3], Ruck et al. [4,5], Arbeiter et al. [6]. Turbulent flow and heat transfer of cooling channels rib-roughened by upstream directed, truncated 60° V-shaped ribs and transverse ribs with various rib shape were analyzed numerically and experimentally. The rib designs were developed under consideration of conventional manufacturing aspects. Here, the results showed that the best cooling performance was obtained for truncated 60° V-shaped ribs with square rib cross section and the local heat transfer can be improved by rib shape modifications. In the present paper, Large-Eddy-Simulation (LES) was performed to investigate the thermal-hydraulic performance of cooling channels structured by truncated fully attached and semi-detached 60° V-shaped ribs and by spherical dimples.

2. Methods

2.1 Computational Domain

The turbulent flow and heat transfer were determined in a FW cooling channel model of DEMO. The intensively heated channel wall was structured by V-shaped ribs and dimples, as depicted in Fig. 1. a and b.

V-shaped ribs - The rib-height of the upstream directed truncated V-shaped rib was $e = 0.833$ mm. The rib-length-to-channel-width ratio was $l_e/W = 0.73$ and the channel blockage by the rib was 6.38 %. The front inclination angle was 60° and the rear inclination angle was 69.2 ° leading to a diminution of the rib in spanwise direction. For the semi-detached ribs, the gap-height-to-rib-height ratio was $c/e = 0.1$ and the width of the gap fillet was 6.11 mm and 3.06 mm respectively. The channel width and height were 12.5 mm each and the inner radius of the round-edged channel corners was 1.67 mm. The thickness of the plasma-facing wall was 2.1 mm and the thickness of the breeding-zone-facing wall was 7.4 mm, leading to a FW thickness of 22 mm.

Dimples - The spherical dimples were positioned in a staggered array on one channel wall. A total of 8 rows of dimples are employed in spanwise direction. The ratio of dimple depth to dimple print diameter was $D_d/d = 0.3$. The distance between the dimple centers was $s_1 = 1.2$, 1.5 and 2.0 in streamwise direction and $s_2 = 1.5$ in spanwise direction. The channel cross section was 15 x 15 mm^2 and all channel corners were round-edged with an inner radius of 2 mm. The total thickness of the FW was 30 mm, the thickness of breeding-zone-facing wall was 12 mm and the thickness of the plasma-facing wall was 3 mm.

author's email: sebastian.ruck@kit.edu

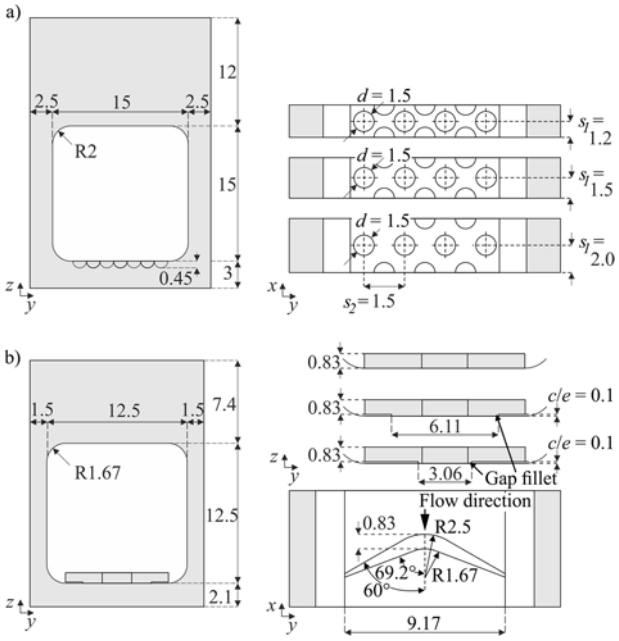

Fig. 1. Geometric details of a) the dimpled channels and b) the rib-roughened channels. All dimensions are given in mm.

The attached ribs and dimples are feasible for manufacturing by Electrical-Discharge-Machining or additive manufacturing technologies of Metal-Powder-Application in combination with machining as well as continuous production by Selective-Laser-Melting as described by Neuberger et al. [7,8]. The manufacturing of semi-detached ribs requires additional machining, i.e. wire cutting. However, the design of the semi-detached ribs was attributed to the cost efficient ladder-like rib manufacturing concept [5]. In this context, the gap between the rib and the channel wall represents common manufacturing tolerances.

LES were performed with periodic boundary conditions in streamwise direction. The computational domain including the solid structure and the fluid domain is displayed in Fig. 2. For the rib-roughened cooling channels, each computational contained one rib-element and the length in streamwise direction was L = 8.33 mm leading to a rib pitch of p/e = 10. For the dimpled channels, the streamwise length L of the computational domain varied with the distance between the dimple rows.

The fluid mesh sizes of the periodic computational domain were in the range from $11.5 \cdot 10^6$ to $13.0 \cdot 10^6$ hexahedral cells for the rib-roughened channels and in range from $14.7 \cdot 10^6$ to $15.8 \cdot 10^6$ hexahedral cells for the dimpled structured channels. The LES quality conditions of a non-dimensional maximum cell size in streamwise direction $\Delta x^+_{max} \leq 40$ and in span- and crosswise direction $\Delta y^+_{max} \approx \Delta z^+_{max} \leq 25$ were meet for the most part of all computational domains. The mesh was refined in flow regions close to the channel walls. The region from $z^+ = 5$ to $z^+ = 70$ was resolved by 20 nodes and the viscos sublayer in the range of $z^+ < 5$ was resolved by 5 nodes with a wall-normal first cell spacing of $\Delta z^+ < 1$.

2.1 Simulation Details

Simulations were performed for incompressible helium-gas with an operating pressure of p_{opt} = 8.0 MPa

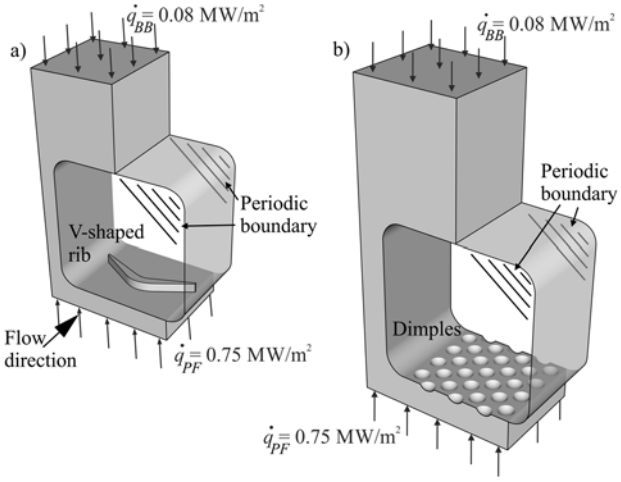

Fig. 2. Sketch of the computational domain for the a) ribbed channel and b) the dimpled channel.

at a Reynolds number of $Re = 1.05 \cdot 10^5$. Depending of the channel cross section of the differently structured channels, the corresponding mass flow rate was $\dot{m}$ = 0.0490 kg/s and 0.0407 kg/s respectively. The inlet bulk temperature was T_{in} = 340 °C. Non-slip conditions were applied on all channel walls. A constant heat flux density of $\dot{q}_{PF}$ = 0.75 MW/m² was applied on the plasma-side-facing FW surface and the heat source from the breeding-blanket modules were approximated by applying a flux density of $\dot{q}_{BB}$ = 0.08 MW/m² on the breeding-blanket FW surface as displayed in Fig. 2. Symmetry conditions were employed on the outer side, rear and front walls of the solid domain. Averaged material parameters approximated for the expected temperature range were used for Helium [9] and EUROFER steel [10]. For EUROFER steel the specific heat capacity was c_p^E = 727 J/(kg·K), the thermal conductivity was κ^E = 29.7 W/(m·K) and the density was ρ^E = 7617 kg/m³. For Helium, the specific heat capacity was c_p^{He} = 5196.54 J/(kg·K), the thermal conductivity was κ^{He} = 0.2537 W/(m·K), the dynamic viscosity was $\mu^{He} = 3.2859 \cdot 10^{-5}$ kg/(m·s) and the density was ρ^{He} = 6.277 kg/m³. The time step was defined by the smallest cell size in streamwise direction, the corresponding maximum flow velocity and a Courant-Friedrich-Number of CFL < 0.9 for all flow simulations.

FLUENT 19.0 was used for the present study [11]. The subgrid-scales were determined by the dynamic Smagorinsky model and the subgrid-scale Prandtl number was Pr_{SGS} = 0.85. The governing flow and energy equations were discretized with the finite volume method and were solved by the pressure-based segregated solver. For the pressure-velocity field coupling the SIMPLE algorithm was applied. The convective terms of the momentum and energy equation were approximated by the bounded central differencing scheme and pressure terms were determined by a second order scheme. The gradients were Least-Square-Cell-Based approximated and the bounded second order implicit scheme was applied for the temporal integration. A computationally developed state was reached after 93, 74 and 80 flow-throughs over the periodic domain for the dimpled channels and after 126, 111 and 136 flow-throughs over the periodic domain for the rib-roughened channel.

2.2 Data evaluation

After a computationally developed state was reached, data were time averaged over 1.5 x 10^4 time steps for the rib-roughened channel and over 2.0 x 10^4 time steps for the dimpled channel. The local heat transfer coefficient was calculated from

$$HTC(\vec{x}) = \dot{q}(\vec{x})/\big(T_W(\vec{x}) - T_B(x)\big), \quad (1)$$

with the local wall heat flux density $\dot{q}(\vec{x})$, the local wall temperature $T_W(\vec{x})$ and the local fluid bulk temperature

$$T_B(x) = T_{in} + x \cdot \dot{Q}_{tot}/\big(\dot{m} \cdot c_p^{He} \cdot L\big). \quad (2)$$

Here, x is the streamwise coordinate starting at the beginning of the computational domain and $\dot{Q}_{tot}$ is the total power transferred by $\dot{q}_{PF}$ and $\dot{q}_{BB}$. The averaged heat transfer coefficient was determined by

$$\overline{HTC} = \overline{\dot{q}}/\big(\overline{T_W} - \overline{T}_B\big), \quad (3)$$

with the surface averaged heat flux density $\overline{\dot{q}}$ and the surface averaged wall temperature $\overline{T_W}$ of the structured surface. The averaged fluid bulk temperature was

$$\overline{T}_B = (2 \cdot T_{in} + \dot{Q}_{tot}/\dot{m} \cdot c_p^{He})/2. \quad (4)$$

The local heat transfer coefficient and pressure drop (PD), respectively, was normalized by a smooth channel heat transfer coefficient HTC_0 and pressure drop PD_0 determined from the Gnielinksi Nusselt number correlation [9] and from the Petukhov friction factor correlation [11] for fully developed turbulent pipe flow.

3. Results

3.1 Global heat transfer and pressure drop

The averaged HTC ratio is plotted against the PD ratio in Fig. 3. The HTC ratio and the PD ratio are 2.6-2.8 and 5.4-5.8 for the V-shaped ribs. The results show, that the present V-shaped ribs produce higher heat transfer enhancement than the V-shaped ribs previously tested and smaller pressure drop than attached or detached V-shaped ribs with a rib-length-to-channel-width ratio of $l_e/W = 1.0$ [3,5]. The semi-detached ribs with the small gap fillet causes the highest global heat transfer enhancement, but the pressure drop is comparable to the fully attached rib. For the dimples, the HTC and the PD are increased by the factor of 1.31-1.38 and of 1.0-1.11 when compared to smooth channel flow. The heat transfer enhancement increases with the distance between the dimple centers: the closer the dimples, the higher the heat transfer.

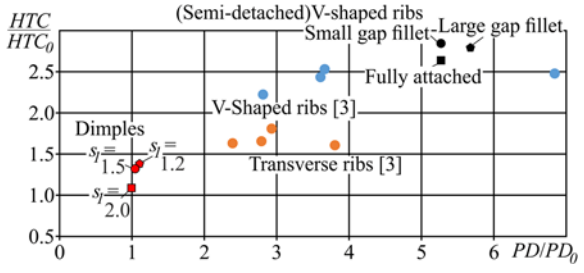

Fig. 3. Normalized global heat transfer coefficient ratio vs normalized pressure drop.

Evaluating the performance [3] of the different cooling channels reveals that the best cooling performance of the presented surface structures is provided by the semi-detached V-shaped with the small gap fillet, which is comparable to cooling performance of fully attached ribs with square rib cross section. The cooling performance of dimples is better than that of transverse ribs [3], but worse than that of the V-shaped ribs investigated.

3.2 Local heat transfer

HTC distributions are displayed in Fig. 4. Regions local heat transfer reduction with $HTC/HTC_0 < 1$ are colored gray. Local heat transfer deterioration occurs at the rear surface and immediately behind the rib for the attached and semi-detached rib design due to the characteristic flow pattern of V-shaped ribs. The regions of $HTC/HTC_0 < 1$ are comparable for the ribs investigated, but significant smaller than for V-shaped ribs with square cross section [3]. Semi-detaching the rib from the wall induces a gap flow beneath the ribs, which increases the heat transfer additionally [12]. Thus, regions of reduced heat transfer are narrowed in lateral direction and regions of high heat transfer occur at the lower rib leading edges.

The dimpled surfaces show typical HTC distribution. The HTC ratio is low in the upstream dimple halves due to the recirculation region located beneath the flow separated from the upstream rims. The HTC ratio increases further downstream and reaches a maximum near the downstream rim of each dimple. Local heat transfer peaks occur on the surface downstream of the dimples. The heat transfer enhancement is attributed to the impingement/reattachment of the shear layers generated from the detached flow across the dimples and to the unsteady vortical flow motion shed from the dimples [13,14]. Unlike from previous studies, it was found for all dimple configurations investigated, that regions of $HTC/HTC_0 < 1$ are expanded over the complete upstream dimple halves. Thus, reduced heat transfer occurred for a large part of the channel wall.

4. Conclusion and Outlook

The present results and previous studies about turbulent flow and heat transfer in structured cooling channels [3-6] showed, that rib-structuring can yield high heat transfer coefficients which are required for helium cooling in thermally highly loaded blanket components. Local heat transfer deterioration and the pressure drop increase can be reduced by shape optimization.

The results revealed that semi-detaching the V-shaped ribs from the wall provides additional heat transfer and increases the cooling performance. Local heat transfer deterioration was not avoided by the semi-detached ribs, which was found for fully detached transverse ribs [12,15], but the regions were smaller than for V-shaped ribs with square cross section. Compared to smooth channel flows, the heat transfer of the dimpled channels was more increased than the pressure drop. However, regions of $HTC/HTC_0 < 1$ were expanded over each upstream dimple half which can lead to high wall temperatures and, thus, to reduced component life time.

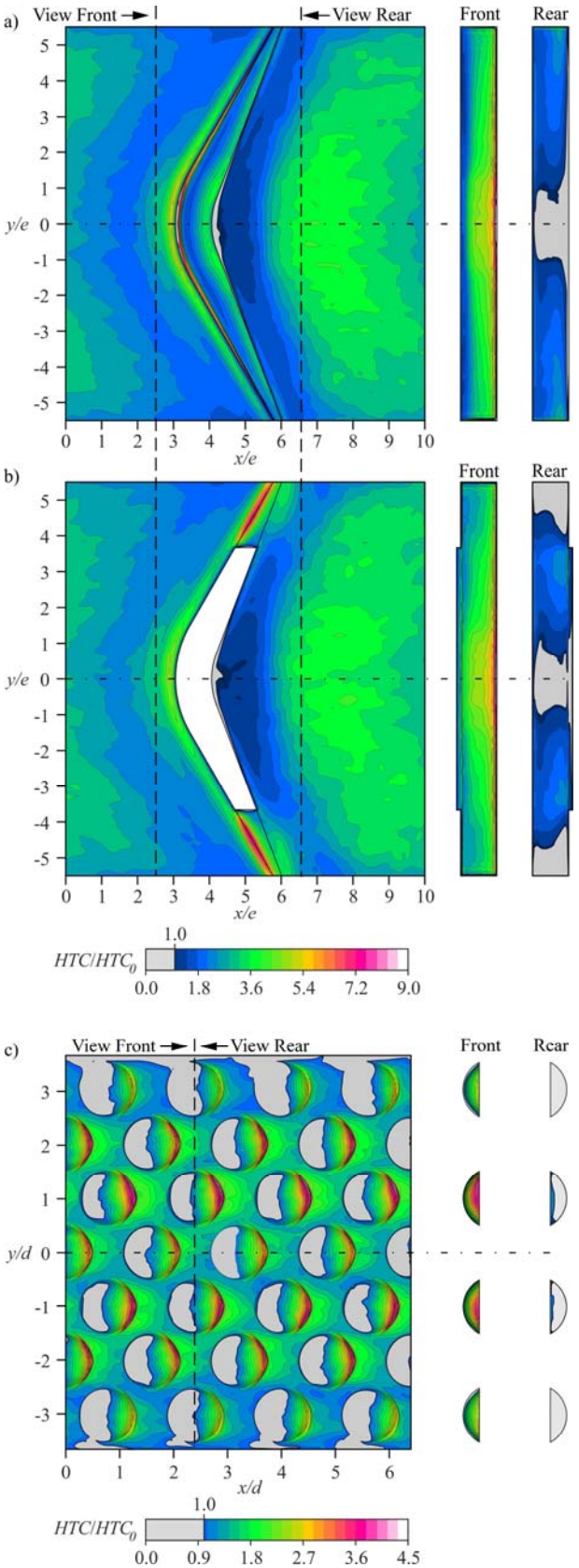

Fig. 4. Normalized local heat transfer coefficient of the a) fully attached rib, b) the semi-detached rib with the large gap fillet and c) the dimpled surface with s_1 = 1.2. Gray areas highlight possible 'hot spot' regions where $HTC/HTC_0 < 1$.

Acknowledgments

This work has been carried out within the framework of the EUROfusion Consortium and has received funding from the Euratom research and training programme 2014-2018 under grant agreement No 633053. The views and opinions expressed herein do not necessarily reflect those of the European Commission.

References

[1] R. Wenninger, R. Kemp, F. Maviglia, H. Zohm, R. Albanese, R. Ambrosino, F. Arbeiter, J. Aubert, C. Bachmann, W. Biel, E. Fable, G. Federici, J. Garcia, A. Loarte, Y. Martin, T. Pütterich, C. Reux, B. Sieglin, P. Vincenzi, DEMO Exhaust Challenges Beyond ITER, Proceedings of the 42nd EPS Conference on Plasma Physics, Lisbon, Portugal (2015).

[2] R. Wenninger, F. Arbeiter, J. Aubert, L. Aho-Mantila, R. Albanese, R. Ambrosino, C. Angioni, J.-F. Artaud, M. Bernert, E. Fable, A. Fasoli, G. Federici, J. Garcia, G. Giruzzi, F. Jenko, P. Maget, M. Mattei, F. Maviglia, E. Poli, G. Ramogida, C. Reux, M. Schneider, B. Sieglin, F. Villone, M. Wischmeier, H. Zohm, Advances in the physics basis for the European DEMO design, Nuclear Fusion 55 (2015) 1-7.

[3] S. Ruck, F. Arbeiter, Detached eddy simulation of turbulent flow and heat transfer in cooling channels roughened by variously shaped ribs on one wall, International Journal of Heat and Mass Transfer 118 (2018) 388-401.

[4] S. Ruck, S. Köhler, G. Schlindwein, F. Arbeiter, Heat transfer and pressure drop measurements in channels roughened by variously shaped ribs on one wall, Experimental Heat Transfer 31(4) (2018) 334-354.

[5] S. Ruck, B. Kaiser, F. Arbeiter, Thermal performance augmentation by rib-arrays for helium-gas cooled First Wall applications, Fusion Engineering and Design 124 (2017) 306-310.

[6] F. Arbeiter, C. Bachmann, Y. Chen, M. Ilić, F. Schwab, B. Sieglin, R. Wenninger, Thermal-hydraulics of helium cooled First Wall channels and scoping investigations on performance improvement by application of ribs and mixing devices, Fusion Engineering and Design 109–111(B) (2016) 1123–1129.

[7] H. Neuberger, J. Rey, A. von der Weth, F. Hernandez, T. Martin, M. Zmitko, A. Felde, R. Niewöhner, F. Krüger, Overview on ITER and DEMO blanket fabrication activities of the KIT INR and related frameworks, Fusion Engineering and Design 96–97 (2015) 315–318.

[8] H. Neuberger, J. Rey, F. Arbeiter, F. Hernandez, S. Ruck, M. Rieth, C. Köhly, L. Stratil, R. Niewöhnere A. Felde, Evaluation of conservative and innovative manufacturing routes for gas cooled Test Blanket Module and Breeder Blanket First Walls, Same Issue

[9] VDI e. V., VDI Heat Atlas, Springer-Verlag Berlin Heidelberg (2010).

[10] RCC-MRx DMRx 10-115 A3.Gen et A3.19AS Eurofer. Afcen (2010)

[11] Petukhov, B.S., Heat transfer and friction in turbulent pipe flow with variable physical properties, Advances in Heat Transfer 6 (1970) 523.

[12] J. Ahn, J.S. Lee, Large eddy simulation of flow and heat transfer in a channel with a detached rib array, International Journal of Heat and Mass Transfer 53 (2010) 445-452.
[13] G.I. Mahmood, M.L. Hill, D.L. Nelson, P.M. Ligrani, H.-K. Moon, B.Glezer, Local Heat Transfer and Flow Strucutre on and Above a Dimpled Surface in a Channel, Journal of Turbomachinery 123 (2001) 115-123.
[14] N.K. Burgess, P.M. Ligarni, Effects Of Dimple Depth on Channel Nusselt Numbers and Friction Factors, Journal of Heat Transfer 127 (2005) 839-847.
[15] E. Marumo, K. Suzuki, T. Sato, Turbulent heat transfer in a flat plate boundary layer disturbed by a cylinder, International Journal of Heat and Fluid Flow 6(4) (1985) 241-248.